1 Connectivity in Urbanscapes Can Cause Unintended Flood Impacts from 2 **Stormwater Systems** 3 Vinh Ngoc Tran¹, Valeriy Y. Ivanov^{1*}, Weichen Huang¹, Kevin Murphy¹, Fariborz Daneshvar^{2,3}, 4 Jeff H. Bednar⁴, G. Aaron Alexander⁵, Jongho Kim⁶, Daniel B. Wright⁵ 5 6 ¹Department of Civil and Environmental Engineering, University of Michigan, Ann Arbor, MI 48109, 7 **USA** 8 ²Ocean and Hydrologic Modeler at National Oceanic and Atmospheric Administration (NOAA) National 9 Ocean Service, Office of Coast Survey (NOS/OCS), Silver Spring, MD 20910, USA 10 ³Ocean and Hydrologic Modeler at Earth Resources Technology (ERT), Laurel, MD 20707, USA 11 ⁴Macomb County Public Works Commissioner Candice S. Miller, Clinton Township, MI 48036, USA 12 ⁵Department of Civil and Environmental Engineering, University of Wisconsin-Madison, Madison, WI 13 53706, USA 14 ⁶School of Civil and Environmental Engineering, University of Ulsan, Ulsan 44600, South Korea 15 16 December 01, 2023 17 18 19 Corresponding author: *Valeriy Y. Ivanov; Email: ivanov@umich.edu; ORCID: 0000-0002-20

21

5208-2189

23 Urban flooding is intensifying worldwide, presenting growing challenges to urban communities. 24 We posit that most of the flood management solutions currently employed are local in nature and 25 fail to account for ways in which the space-time connectivity of floods is exacerbated by built 26 infrastructure. We examine the 2014 flood in Southeast Michigan to identify key factors 27 contributing to urban flooding and explore the implications of design choices on inundation. 28 Findings reveal that stormwater infrastructure that neglects flood spatial connectivity can be 29 ineffective in mitigating floods, leading to inundation even in the absence of local rainfall. 30 Different configurations of network connections—including interfaces with natural channels— 31 can significantly impact upstream surcharge, overflowing manholes, and inundation conditions. 32 These results emphasize the need to consider interconnectedness of flood processes in urban 33 watershed systems to mitigate limitations inherent in the design of flood control and warning 34 systems, in order to enhance urban flood resilience. 35 **Keywords**: urban flood, flood connectivity, stormwater system, extreme rainfall, surcharge 36 37 38

22

Abstract

Main

Climate change is increasing the likelihood of flooding ^{1,2} with often disastrous impacts, particularly in urban areas ^{3,4}. Flood-related global economic losses reached a staggering \$651 billion (USD) between 2000 and 2019 ⁵. The United States has been particularly affected, with floods causing 1,782 fatalities, damages exceeding \$102 billion, and affecting 99% of U.S. counties since 2000 ⁶⁻⁸. The growing impacts of flood events across the U.S. and global will continue to rise, with losses projected to soar by a factor of twenty by the end of the 21st century ⁹. These increasing impacts are driven not only the increasing severity of extreme rainstorms, but also rapid urbanization ¹⁰, booming population densities, and the dramatic expansion of highly connected transportation and infrastructure networks in flood-prone areas ^{11,12}. Rapid urbanization has substantially altered the natural water cycle through the proliferation of impervious surfaces, inhibiting rainfall infiltration and resulting in elevated surface runoff ¹³. The disruption of natural drainage pathways has rendered urban areas increasingly susceptible to inundation. Consequently, numerous major cities globally have witnessed a rise in the frequency and severity of flood events, as urbanization outpaces upgrades to flood mitigation infrastructure, oftentimes referred to as stormwater systems ¹⁰.

Stormwater systems play an essential role in cities globally (Supplementary Fig. 1). Stemming from advances in science and technology over the past decades, a new generation of flood mitigation infrastructure such as Green-Blue infrastructure systems (GBI) are perceived as the future of urban flood management, designed to replace traditional "grey" approaches ¹⁴. GBI refers to an integrated approach that combines "green" infrastructure solutions such as permeable pavements, rain gardens, and green roofs with "blue" infrastructure elements (or low-impact development) such as constructed wetlands, detention ponds, and restored floodplains. Despite the apparent merits of GBI (e.g., eco-sustainability and climate change resilience) ^{15,16}, they are costly, require a longer implementation period, and necessitate continuous maintenance to ensure efficient drainage and retention capabilities, with the continued reliance on grey infrastructure ^{17,18}. Therefore, grey infrastructure persists as the primary approach for mitigating urban flooding ^{17,19,20}.

The repetitive damages caused by urban flooding have raised questions regarding the efficacy of costly drainage systems, whether grey or GBI. For example, the United States spends \$7-10 billion dollars annually for the construction and renovation of stormwater systems, with larger expenditures needed over the long-term ²¹. With the generally poor state of aging infrastructure in the U.S. ²², even moderate rainfall events (the return period of about 10 years) ^{23,24} can exceed the capacity of drainage systems ⁸. While current inadequacies stem partly from outdated stormwater design standards ^{25,26}, we posit that it is also due to insufficient understanding of "*flood connectivity*" within urban landscapes, defined as a complex interplay of flooding mechanisms (Fig. 1) and drainage pathways within urban settings, arising from the spatiotemporal distribution of hydraulic head (the term used to describe the summed potential, kinetic, and pressure energies of stormwater flows). This flood connectivity encompasses the interactions and interdependencies between runoff, surface and subterranean sewer and drainage systems, rivers and other natural and built water bodies, and infrastructure components (e.g., buildings and roadways) that can, by design or in an unintend, convey stormwater during floods. Although numerous studies have been

conducted in recent decades focusing on understanding urban flooding (see Supplementary Table 1 for a detailed literature review), most previous studies have focused on a few specific, isolated physical phenomena, such as assessing the impact of infrastructure and rainfall on flooding, or case-study specific aspects of water exchange between drainage systems and surface flows. Therefore, a comprehensive exploration of flood connectivity in complex urban areas and a holistic synthesis of process interactions remain lacking.

Insufficient appreciation of flood connectivity can be showcased with outdated and oversimplified stormwater system design guidelines ^{22,27}. For example, American Society of Civil Engineers (ASCE) stormwater design guidelines were last revised in 2006 (GUIDE2006 hereafter) ²⁸. While offering an extensive set of drainage network design criteria, GUIDE2006 do not adequately reflect the ways that drainage system interconnectedness that can create vulnerabilities through the aggregate "network effects" of localized engineering solutions. Additionally, modeling tools employed in engineering design practices are outdated and lack the capability to describe the coupled dynamics between flows over the land surface, through natural and artificial surface channels, and through sewer systems. Similar deficiencies in design practices can be found worldwide ²⁸⁻³³, and exist despite the availability of more modern modeling tools that are capable of performing such sophisticated simulations. These practices have impacted scientific research focusing on the optimization of drainage systems, as most studies relied solely on the simplified one-dimensional models that simulate water conveyance within sewer systems, while neglecting interactions with surface water (see Group 3 in Supplementary Table 1 containing relevant literature review). Such model limitations may result in poorly-informed design of drainage systems and may compromise the urban flood resilience and prevention capacities ^{4,34,35}.

State-of-the-science urban flood modeling can accurately simulate the motion of flood waves over the surface and within stormwater infrastructure, while accounting for complexities of surface conditions (vegetation, roads, bridges, buildings, etc.) ³⁶⁻³⁸. Augmented with the growing volumes of high-resolution geospatial data on urbanscapes, it is now possible to explore flooding behaviors in urban environments with far fewer simplifying assumptions. As pointed out above, previous studies have primarily focused on model developments of specific physical processes ³⁷ and thus lacked comprehensive insights on the connectivity of floods in urban domains as shaped by the natural drainage elements and grey infrastructure. This warrants further research to advance such understanding. By investigating flood propagation through a complex urban environment with multiple process interactions, our study provides novel insights into emergent flood behaviors shaped by both natural and man-made drainage systems. Knowledge gained and capabilities demonstrated in this research can aid in improving sustainable and resilient approaches to address intensifying global urban flood hazards.

Specifically, we investigate (1) What is the nature of complexity of flood connectivity in urban landscapes? (2) Can sewer systems exacerbate urban floods? We hypothesize that: (i) in certain conditions, the connectivity via stormwater infrastructure can lead to flooding in a particular location, even in the absence of "local precipitation; and (ii) improper positioning of stormwater drainage outlets and curb inlets (called as manholes hereafter) can exacerbate flooding.

121 Results

122

Flood of 2014 in Southeast Michigan

123 We present a case study that demonstrates how engineering design infrastructure interacts with 124 runoff drainage processes that have different spatial scales of origin, including both local scales, 125 typical of engineering design, and larger scales that connect upstream and downstream drainage 126 conditions. The study has been carried out for a highly urbanized watershed in Southeast Michigan 127 that has multiple conventional elements of grey infrastructure designed to deliver storm runoff to 128 nearby channels. We designed the study focusing on a single exemplary extreme storm on 11 129 August, 2014 (referred to as STORM2014 hereafter) that struck Southeast Michigan causing 130 catastrophic flooding. The storm was termed a 1-in-100-year event with rainfall totals between 4 131 to 6 inches in four hours ³⁹. The economic costs of the storm were significant, with a total of over 132 US \$1.1 billion damages to over 118,000 homeowners and businesses 40, translating to the largest 133 flood-related disaster that the Federal Emergency Management Agency (FEMA) identified during 134 2014. The area was declared a federal disaster zone in that September ⁴⁰. The study focus is on the 135 Warren area situated within the confines of the inner-ring Detroit suburb of Madison Heights and 136 approximately 8.8 km² in size (Fig. 2a-b). This region is considered to be a part of the Red Run 137 watershed dissected by a network of diverse drainage elements such as open channels (i.e., Bear 138 Creek, Fig. 2b and Supplementary Fig. 2), culverts, underground stormwater conveyance systems, 139 and their outlets (outfalls, Fig. 2b-c). In contrast to this drainage complexity, the National Flood 140 Hazard Layer from FEMA (Fig. 2b) shows 1% or 0.2% annual probability floodplains mainly 141 confined to the vicinity of Bear Creek 41. Nonetheless, throughout the STORM2014 event, the 142 majority of the Warren area, comprising residential neighborhoods and major roadways, 143 experienced profound inundation as depicted in the simulation results in Fig. 2d. Specifically, 58% 144 of the domain area was affected by severe flooding, with water levels exceeding 0.5 meters 145 reported by eye-witnesses in the area of the General Motors production facility (Supplementary 146 Fig. 2b). Since the area typifies urban watersheds connected to a larger drainage system, this 147 domain was selected for an analysis of interactions of urban flooding mechanisms. To replicate 148 historical flood events, we gathered an extensive array of data of high accuracy and spatial 149 resolution that influence the flood response in this area, including topography, landuse/land cover, 150 road networks, buildings, stormwater systems, and open channels. Notably, we conducted field 151 surveys to validate and refine the data, particularly regarding the locations of drainage outfalls, 152 where strong interconnections exist between the drainage system, open channels, and ground 153 surfaces. Further details on the specific data used and the model configurations are provided in 154 Methods.

No local rain – but flooding

155

156

157

158

159

160

161

The design of stormwater system in GUIDE2006 are based on the rainfall scenarios that represent different levels of precipitation that can cause flooding if the stormwater infrastructure is unable to accommodate the influx of runoff quickly enough. In other words, GUIDE2006 assumes that rainfall occurrence is a pre-requisite for flooding. However, we show that even in the absence of rainfall in local runoff source areas, runoff from heavy rain *outside* of their boundaries can still cause inundation due to the spatial hydraulic connectivity facilitated by the stormwater

infrastructure. Results in Fig. 2e highlight that a substantial portion of the studied area is susceptible to flooding: water exceeds 0.1 meters in depth over about 75% of the area, with 27% having depth over 0.5 meters). Such an outcome indicates how spatial connectivity of flood processes can alter a local perception of flood vulnerability conditions. Specifically, scenarios with intense precipitation only in neighboring areas must be considered when assessing flood risks and planning mitigation for a region of interest, even in the absence of rainfall occurring locally within that area.

One source of flooding in this "no local rain" situation can be attributed to the increased water levels in open channels causing the well-known phenomenon of fluvial flooding ("FC1" in Fig. 1). Under this mechanism, the water levels exceed the confines of the riverbanks, and streamflow spills into floodplain areas. Additionally, simulated results show that runoff from the surrounding land areas (where rainfall occurs) can flow along roadways into the Warren area, leading to a localized pluvial flooding denoted by "FC2" – (Fig. 1). A third likely cause identified is related to the backwater surcharge through the stormwater pipe network and their catch basins in source areas. Specifically, extreme water levels within open channels induce backwater flow at stormwater outfalls, causing a significant surge of reverse flow into topographically upstream source areas of the drainage system, leading to surcharge at manholes and flooding in areas that did not experience rainfall. This flooding mechanism reflects concept "FC3" - infrastructure-induced flooding that can impact areas distant from open channel.

Indeed, the results of explicit modeling of flood connectivity present evidence that stormwater networks design with a "local mindset" may severely fail. Not only can they become inadequate to accomplish their designated task to drain stormwater, but they can even reverse stormwater systems' work to aggravate flooding due to sewer surcharge in residential areas that do not experience rainfall (Fig. 2e). The spatial connectivity of flooded urbanscape may thus lead to the hydraulic head distribution expansion of inundation into regions that are distanced from a river or do not experience extreme rainfall.

No backwater flow into outfalls – but heavier local flooding

The location, invert elevation, and size of outfalls and their associated sewer pipes play a major role in determining the drainage capacity of a stormwater collection system. As stipulated in GUIDE2006, the entire volume of generated runoff within the system is assumed to freely flow out from outfalls. While this permits an assessment of the maximum drainage capacity, such an assumption may underestimate the influence of flood connectivity at outfalls, e.g., the distribution of hydraulic head in open channels or storage tanks. If the hydraulic head at the outfall section generated by the passing flood wave in the channel exceeds the hydraulic head in the stormwater system, then the backwater flow commences and channel water will flow into the sewer system, impeding stormwater drainage and possibly even causing surcharge at upstream locations. The lack of consideration of flood connectivity in complex urbanscapes may lead to incorrect assessments of system drainage capacity and therefore inaccurate representation of possible inundation levels at sites requiring flood protection.

We examined how accounting for flood connectivity or lack thereof may impact flood levels. Specifically, the former case (referred to as the "Integrated" outfalls) accounted for the hydraulic coupling of water levels in open channels at the outfalls, mimicking the real-world flood condition to the best of our abilities. In the latter case ("Controlled"), all stormwater at the outfalls is assumed to freely discharge into the receiving channel of Bear Creek, i.e., the outflow is controlled to have the rate of a pipe with a free overall downstream condition, not impeded by the presence of the receiving water body. Comprehensive hydrodynamic modeling of these two distinct scenarios of outfall functioning reveals peculiar results. Notably, with the outfalls that are hydraulically disconnected (i.e., the "Controlled" case) from the rest of the flooded watershed, the resultant flooding is more extreme as compared to that of the integrated outfall case which facilitated backwater effects (Figs. 2d, f). Specifically, in the areas near the outfalls at the Bear Creek channel, inundation levels for the "Controlled" case exceeded the "Integrated" case by over 0.1 meters (Fig. 2g and 3a, 3b-c). This result can be explained by the considerable drainage from the "Controlled" sewer system discharging into the open channel: water levels at the outfall sites thus tend to be higher and cause more severe flooding in the nearby areas. In contrast, in the more realistic "Integrated" case, if the water level in the channel exceeds the hydraulic head of the stormwater system at the outfall location, backwater flow will occur and water from the open channel will flow into the sewer system. This results in lower water levels in near outfall areas experiencing backwater, leading to reduced flooding in the "Integrated" case. Conversely, with large discharges entering the sewer system, upstream areas (such as in the southern region) can be impacted when the sewer's rainwater intake capacity is reduced, potentially increasing flooding due to slower drainage.

201

202

203

204

205

206

207

208

209

210

211

212

213

214

215

216

217

218

219

220

221

222

231

232

233

234235

236

237

238

239

240

241

242

223 The neglect of connectivity between a sewer system and adjacent flooded areas and consequent 224 backwater effects can *overestimate* flood levels. This can potentially result in poor design of the 225 number, positioning, and dimensions of manholes, pipes, and outfalls. Larger sewers and outfall 226 dimensions can facilitate rapid drainage, yet they can also allow rapid backflow. As shown in Figs. 227 3d-e, the large outfall (with a diameter of 3.8 m) can discharge high flows (up to 40.9 m³/s) in the 228 "Controlled" case, while the backflow into the sewer can be up to 63.5 m³/s in the "Integrated" 229 case. The smaller outfall (with the diameter of 0.3 m) had lower discharge and backflow (up to 9.7 230 and 16.7 m³/s for the controlled and integrated cases, respectively).

It is still far from being standard engineering practice to realistically simulate flooding with coupled overland- and pipe- flow models, such as the one used in this study (i.e., results shown in Fig. 2). Instead, engineers mainly rely on simplified stormwater models (e.g., one-dimensional channel flow models coupled with conceptual/lumped rainfall-runoff modules ^{28,30-33,42,43}. In such formulations, the total discharge from outfalls is assumed to entirely "disappear" (or become accommodated by a stormwater storage such as pond or tank) rather than flow into open channels. Water levels in open channels (at outfall locations or elsewhere) will thus remain unaffected and no backwater effect can occur. The assumption that stormwater discharge vanishes after discharging through outfall clearly can have a strong impact on flood level assessments, and can misjudge drainage system performance. Specifically, inundation levels are broadly *underestimated* across the study area (especially near open channels) by up to 20 cm, as compared to the more real-world like "HR-Integrated" case (Supplementary Fig. 3a, b). These estimates indicate that

243 even assumptions for outfalls can lead to significantly different assessments of stormwater system

244 performance. This highlights that the lack of appreciation of flood connectivity may result in

245 poorly informed stormwater system designs.

246

256

270

271

272

273 274

275

276

277

278

279

280

281

282

More overflowed manholes – but lower surcharge amounts

247 Different outfall configurations should produce distinct differences in the surcharge in catch basins.

248 In principle, when the sewer system simultaneously receives a significant influx of water from

249 both the ground surface through manholes in source areas and from the open channel through

250 outfalls, this can induce higher surcharge and a larger number of surcharging manholes in low-

251 lying areas (i.e., where low hydraulic head is expected). The case study results only partially align

252 with this conjecture, showing that accounting for backwater effects (the "Integrated" case) results 253

in surcharging in a slightly larger number of manholes (27 versus 25), as depicted in Figs. 2d and

254 2f. Figs. 3f-g indicate that the surcharge rates in manholes near the outfalls are comparatively

255 lower as compared to the "Controlled" case (e.g., Manholes #1 and #2). The differences in the

surcharge rates were negligible for manholes farther from the outfalls or at higher elevations

257 (Manholes #3, 4, and 5, Figs. 3h-j).

258 The higher surcharge rates at manholes (e.g., Manhole #1, Fig. 3f near Outfall #2) in the 259 "Controlled" case are attributed to the higher water volumes "injected" into the flooded area from 260 a nearby draining outfall. Such an "injection" leads to larger volumes of water inflow into the 261 adjacent manholes, e.g., Manhole #1 and nearby manholes (see Fig. 2f) and, if paired with a limited 262 drainage capacity of the outfall, (e.g., Outfall #2 that has a small 0.8 m diameter), can exacerbate 263 the surcharge (Fig. 3f-g). These results demonstrate how outfall configuration/drainage capacity 264 can impact an assessment of local flooding conditions. This underscores the complexity and vital 265 importance of flood connectivity for understanding the performance of stormwater infrastructure. 266 Ignoring flood connectivity between land surfaces, infrastructure, and open channels in urban areas 267 can lead to incomplete understanding of how water moves through a complex urban flooding 268 environment. Failing to account for this interconnectedness misinforms engineering design and 269 flood mitigation strategies.

Discussion

Existing evaluations of urban flooding have so far neglected to account for the interactions of complex mechanisms associated with flooding caused by human-engineered stormwater networks ^{22,23,37,38,44-46}. Our results demonstrate that interaction of flooding types – facilitated by the connectivity created by human-engineered infrastructure – is an important aspect of urban flood dynamics. Ignoring such a connectivity may lead to intensified urban floods, especially in regions where river-induced floods meet stormwater infrastructure (Fig. 2d, f), even when rainfall does not occur over the area served by the infrastructure. To expand the applicability of the study findings to a broader range of flooding cases, we conducted simulations for the 14 largest events (including STORM2014, Supplementary Fig. 4) over the past 15 years in the Warren study area (rainfall return periods ≥ 1 year) with outfalls that have hydraulic connection with the receiving channel, thereby mimicking the real-world conditions. The simulation maximum flooded areas are shown in Fig. 4a. Even for the annual flood (i.e., a return period of 1 year), the total area flooded

over 0.5 m is up to 7% of the total area of the Warren area (excluding the area of open channels). With the increase in rainfall intensity (as shown in Fig. 4b for STORM2014), the area of severe flooding and the flood level also increase (Figure 4c). It should be noted that the drainage system in this area is designed to handle runoff resulting from a 10-year storm, with the assumption that all rainfall will be converted to runoff and flow into the drainage system ⁴⁷. However, in reality, not all runoff efficiently concentrates in the drains due to the retention of some water in low-lying areas, causing localized flooding.

Additionally, we carried out simulations for all events to evaluate the impact of the stormwater system on flooding under varying rainfall conditions and outfall configurations, in the same fashion as this was done in the simulation configurations for STORM2014 (Supplementary Figs. 5-17). Generally, the rainfall magnitude certainly influences the performance of the stormwater system, with fewer instances of manhole overflow occurring under lower rainfall intensities. We still observe the same flooding phenomenon implied by the flood connectivity. For instance, the number of overflowing manholes in the HR-Integrated case is higher than in the HR-Controlled case. The case of rainfall in the watershed outside of the Warren area can still cause flooding and overflow at several manholes in that area. Overall, simulation results for 14 rainfall events of different magnitudes corroborate the persistence of analyzed flood dynamics in the case study urban area caused by flood spatiotemporal connectivity.

Another observable outcome is the rapid onset of flooding after rainfall. As depicted in Fig. 4c, impactful flooding with inundation depths exceeding 0.5 meters occurs within a narrow time window following the most intense precipitation (initiating at hour 15:00), within 0.5-1 hour. This signifies that to mitigate flooding, the drainage system must not only store substantial rainwater volumes but also drain rapidly to minimize local water accumulation. However, the influx of water from the surrounding areas or backwater effects at outfalls can exceed pipe and manhole conveyance capacities and thus cause drainage "bottlenecks". Failure to adequately consider flood connectivity can lead to the design of infrastructure (e.g., massive underground storages) that may fail to counter flooding (see results in Supplementary Text 1). Optimization-based approaches are likely required to alleviate the issue of drainage "bottlenecks".

The recognition of the potential hazard imposed by flooding due to its connectivity, even in the absence of rainfall in the design area, is an important but overlooked reality of urban stormwater systems. It is noted that most design guidelines worldwide ^{28,30-33} rely on scenarios with only "direct rainfall" occurring in the area of interest (often uniform), without considering influx/outflux from/to nearby interconnected areas. With flooding waters contributed by sources other than direct rainfall, assessments of drainage capacity can be highly uncertain. Similar to above, stormwater system design may require optimization of its configuration.

In the U.S., FEMA maps require further updates in flood-prone areas, as already highlighted in previous research ⁴⁸⁻⁵⁰. The current perception is that FEMA's hazard maps, which have not been updated for over a decade, are outdated due to climate change and land use alterations ⁴¹. Critically, we show here that FEMA maps are further outdated as methods (modeling and flood concepts) used to generate them do not consider the complexity of flood connectivity, especially in urbanscapes. Hence, flood risk assessments can become particularly unreliable for urban zones

where the different flood processes interact (Fig. 1), compromising their utility. For the specific case study considered here, the simulated water levels during STORM2014 at the two discussed outfall locations were higher than what FEMA maps show for the 0.2% annual flood probability (a 500-year return period). This was also confirmed by eye-witness accounts. This demonstrates the necessity for more accurate models to mimic the spatial interactions of flood mechanisms across rivers, surfaces, drainage systems, and other infrastructure types.

The execution of this study is not without limitations. First, the hydrodynamic model employed, while advanced and sophisticated, is subject to inherent uncertainties arising from physical process simplifications, parameterizations, and input data quality. Secondly, the use of crowdsourced data, such as images from the internet, to estimate flood depths at a few locations introduced subjectivity and uncertainties into the model evaluation process. This arises from the potential misalignment between the timing and locations of the crowdsourced data with the simulation configuration. Thirdly, the study focuses on a single event, and therefore carries the signature of specifics of this case study. The findings have been generalized to highlight study broad level implications but other urban areas with differing topographic, hydrological, and infrastructure characteristics will require similarly detailed analysis to understand the impacts of flood space-time connectivity. These limitations underscore the necessity for further research with diverse case studies and the requirement for observations of inundation depth data and drainage system operational data. Notwithstanding these limitations, the paper presents a novel contribution by accentuating the importance of considering flood connectivity in urban flood mitigation strategies and the potential shortcomings of traditional stormwater management approaches that neglect the interconnectedness of flood processes.

In summary, urban flooding is a result of complex interactions between precipitation, terrain and landuse, surface hydrology, and human infrastructure systems. Disentangling the complex interactions that flood connectivity produces in urbanscapes is imperative for improved urban flood resilience and mitigation. By explicitly analyzing such interactions for a case study with documented flooding issues, this work emphasizes that it is vital to distinguish the distinct mechanisms of fluvial, pluvial, and infrastructure-induced flooding, so that better engineering solutions can be developed. Holistic perspectives encompassing the complete connectivity between all facets of the urban flooding system, rather than compartmentalized viewpoints, need to be prioritized as cities strive to enhance their flood resilience and sustainability.

Methods

330

331

332

333

334 335

336

337

338

339

340

341

342

343

344

345

346

347

348

349

350

351

352

353

354

355

356

Case study and dataset

The main study area, Warren, encompasses the urban domain of the Red Run watershed located in southeast Michigan (Fig. 2a-b). This is a complex urban area with a significant proportion of impervious surfaces. The land use cover obtained from the National Land Cover Database 2019 (NLCD, https://www.mrlc.gov) indicates a predominant presence of developed areas with buildings, driveways, pavements, and parking, with an impervious surface ratio reaching 94.48% (Supplementary Fig. 18). The terrain in this region is relatively flat, with a northward slope adjacent to Bear Creek. According to FEMA reports, some Warren areas fall within the 100 and

500-year flood zones. To ensure a realistic simulation, a substantial amount of digital and field observational data were collected to set up the model accurately.

366 The overall simulation domain encompasses the entire Red Run watershed in which the Warren 367 region is nested (Fig. 2a). This was done to ensure the modeling of spatial flood processes, such 368 surface inflows into the Warren area from other sub-basins and the simulation of flood waves in 369 the Red Run River and its tributaries and their impact on the Warren area. High-resolution 370 elevation data (0.6m resolution) were used to set up the overland flow model (Lidar Point Cloud 371 data kindly provided by the USGS, https://apps.nationalmap.gov/downloader/) (Supplementary 372 Fig. 19a). Land use/land cover data with a 30m resolution obtained from the NLCD were used to 373 estimate roughness parameters for the model. Similarly, impervious surface data with a 30m resolution, also derived from the NLCD, were used to estimate infiltration parameters. It is worth 374 375 noting that other areas within the Red Run watershed also exhibited high impervious surface ratios, 376 ranging mostly between 47% and 95%.

377 Infrastructures (buildings and stormwater systems) play a crucial role in surface flow routing and 378 water drainage of the urbanized areas. The most recent building footprint data were obtained from 379 the Southeast Michigan Council of Governments (https://maps.semcog.org/BuildingFootprints), 380 encompassing a total of 2,128 buildings within the Warren area (Fig. 2b and Supplementary Fig. 381 20). Data on the stormwater system, including manholes, outfalls, and pipes, were collected and 382 compiled in collaboration with the Macomb and Oakland Counties. A total of 21 culverts, 3,417 383 pipes, 3,393 manholes, and 75 outfalls were identified and incorporated into the simulation for the 384 entire Red Run watershed (see Fig. 2a-b and Supplementary Fig. 2).

The rainfall data were extracted from the Detroit City Airport (DET) weather station, which is a part of the Automated Surface Observing Systems network. In addition to the STORM2014 used primarily in our analysis, data for 13 other major rainfall events from 2009 to 2021 were also collected to simulate and assess the impact of variability in rainfall conditions on flooding. All rainfall events were collected over a duration of 24 hours, with rainfall measurements taken at 1-minute intervals and processed into 15-minute intervals (Supplementary Fig. 4). Flow data at the inlet location (see Fig. 2a) of the Red Run watershed were provided by the Clinton River Watershed Council upon request.

Field support for correcting outfall characteristics

394 Outfalls play a crucial role in the stormwater system, as they are strategically designed to receive 395 and discharge the water volume collected by the manholes, minimizing the risk of flooding. To 396 ensure the closest possible simulation to reality, field observations were conducted on January 21, 397 2023, to refine the design, location, and functionality of the two important outfalls in the Warren 398 area (Fig. 2b-c). Both outfalls are situated in the northern part of Warren, with their discharge gates 399 flowing into Bear Creek. These are open-type outfalls that allow water from Bear Creek to flow 400 inside the stormwater pipes if the hydraulic head in the channel is higher than the hydraulic head 401 at the outfall locations. The field measurements included the width of the outfalls, invert and crown 402 elevations, and the bankfull width of Bear Creek around the outfall area.

Urban flood modeling

385

386

387

388

389 390

391

392

393

A coupled model integrating complex hydrologic, hydraulic, and morphologic processes, which has been verified in previous case studies, was used in the research as the high-fidelity urban flood model ^{51,52}. The hydrology module, the TIN - Based Real Time Integrated Basin Simulator (tRIBS), can simulate various hydrological processes such as canopy interception, evapotranspiration from bare soil and canopy, vertical and lateral moisture fluxes in the subsurface, and diverse runoff generation mechanisms (e.g., saturation excess, infiltration excess, perched subsurface stormflow, and groundwater exfiltration) with appropriate inputs of meteorological data, topography, landuse, and soil type data. Taking into account these hydrologic processes enabled a model to simulate the hydrodynamics of overland flow (Overland Flow Model, OFM ⁵³) relying on physically modelled wave velocities within a domain of arbitrary geometric configuration. The OFM model solves the full form of the two-dimensional Saint-Venant equations (i.e., the shallow water equations), which are derived by depth-integrating the Navier-Stokes equations. The governing equations consist of a continuity equation and two momentum equations for two perpendicular horizontal directions:

$$\frac{\partial U}{\partial t} + \frac{\partial E}{\partial x} + \frac{\partial G}{\partial y} = S$$

where U is vector of flow variables, E and G are the flux terms in X and Y direction, respectively, and S is the source vector:

420
$$U = \begin{bmatrix} h \\ uh \\ vh \end{bmatrix}, E = \begin{bmatrix} uh \\ u^2h + \frac{1}{2}gh^2 \\ uvh \end{bmatrix}, G = \begin{bmatrix} vh \\ uvh \\ v^2h + \frac{1}{2}gh^2 \end{bmatrix}, S = \begin{bmatrix} -gh\frac{\partial z_b}{\partial x} - C_Du\sqrt{u^2 + v^2} \\ -gh\frac{\partial z_b}{\partial y} - C_Dv\sqrt{u^2 + v^2} \end{bmatrix}$$

where h represents flow depth, u, v are the flow velocities in x-axis and y-axis directions in the Cartesian system of coordinates, g is the gravitational acceleration constant, i is the net runoff production rate, z_b is the bed elevation, and $C_D = gn^2h^{-1/3}$ is the surface drag coefficient, where n is Manning roughness coefficient. Detailed descriptions of the numerical solution with the finite-volume method can be found in 53 .

The solution appears to be feasible for many scenarios involving overland flow, however, due to numerical considerations, it is necessary to constrain the time-step of the time-explicit finite-volume method by the mesh's smallest cell area, thus presenting a distinct computational problem. For instance, in high-resolution applications, the typical time-step is approximately of the order of $\sim O(10^{-1})$ sec, with a cell size of around $\sim O(10^{1})$ m. Alternatively, by using a time-implicit numerical scheme for solving the shallow water equations, limitations on time-stepping are fewer and the overall number of solution steps is reduced, generating a potential computational benefit; however, this is limited to no greater than one order of magnitude due to the increased need of iterations within each time-step to handle transient flow situations ⁵³...

The EXTRAN module of Storm Water Management Model ⁵⁴ is fully coupled with tRIBS-OFM for simulating a stormwater drainage system. EXTRAN is a one-dimensional (1D) dynamic sewer network model based on 1D Saint-Venant equations. Water transport in conduits and nodes is calculated based on the continuity and momentum equations written respectively as:

439
$$\frac{\partial A}{\partial t} + \frac{\partial q}{\partial l} = 0, \qquad \frac{\partial q}{\partial t} + \frac{\partial (q^2/A)}{\partial l} + gC\frac{\partial H}{\partial l} + gCS_l + gAe_l = 0$$

where l is the distance along the conduit, C is the cross-sectional area of the conduit, A denotes the cross-sectional area of the conduit, Q and Q are the flow rate and hydraulic head, respectively, of water in conduit at time t, S_l denotes the friction slope of the conduit, and e_l is the local energy loss per unit length of conduit.

Surface water calculated from OFM can move into the sewer network through manholes, and, conversely, if the flow of the pipe network exceeds its drainage volume, a reverse (surcharge) flow occurs and becomes the source term for surface water. Drainage refers to the flow of surface water to the manhole, while surcharge refers to the reverse flow of the flow from the manhole to the surface. These bidirectional discharges, drainage and surcharge, can be calculated from the weir or orifice equations by comparing the hydraulic head at the manhole, the ground elevation, and the water depth of the surface water. Specifically, if the hydraulic head at the manhole (H) is lower than the ground elevation (z_b), i.e., $H < z_b$, drainage, q_d can be computed with a weir equation:

$$q_d = c_w w_w h \sqrt{2gh}$$

where c_w is the weir discharge coefficient for manholes and w_w is the width of the weir crest. Conversely, if the hydraulic head at the manhole rises and is greater than the topographic elevation of the ground surface (but the hydraulic head at the manhole is still less than the surface water level), i.e., $H > z_h$, drainage can be calculated by the orifice formula:

$$q_d = c_o A_m \sqrt{2g(h + z_b - H)}$$

where c_o is the orifice discharge coefficient for manholes and A_m is the area of the manhole mouth. Lastly, if the hydraulic head at the manhole exceeds the surface water level, that is, $H > (h + z_b)$, the surcharge, q_{sur} can be calculated according to the orifice formula:

$$q_{sur} = c_o A_m \sqrt{2g(H - h - z_b)}$$

Mesh generation

This research necessitates sophisticated mesh generation to ensure the most accurate and robust simulation outcomes. The intricate process of mesh generation that considers the complex geometry of the urban environment is visually summarized in Supplementary Fig. 21. Primarily, the Hydrology Analysis Tools of the ESRI ArcGIS Package is used to delineate the watershed area (183.6 km²) starting with the high resolution of 0.6m. Subsequently, the ArcGIS tool "Raster2TIN" is used to construct Triangulated Irregular Network (TIN) from the designated watershed boundary. The TIN is capable of representing the terrain's geometrical structure using significantly fewer nodes than the original raster-based landscape representation.

In this study, we focus on the Warren area (Supplementary Fig. 19b), and thus divide it into cells of a considerably smaller size than those outside the region. To do this, we have established a minimum and maximum grid resolution size of 1 and 100 m², respectively, inside the area of Warren; whereas, for the outer parts, the maximum cell size cannot exceed 5,000 m². As a result,

this refinement of the resolution helps reduce the number of nodes and generated cells, thus alleviating the computational burden. Note that the Warren area does not correspond to a headwater catchment, i.e., surface flows and subsurface pipe flows can enter this rectangle-shaped domain from all of its sides.

We incorporated building footprints into the TIN to account for the impact of buildings on flood wave propagation through the urbanscape. Initially, the building footprints were simplified using the "Simplify Polygon" tool in ArcGIS, ensuring that the minimum length of each footprint polygon edge was 5 meters. These simplified footprints were then merged with the TIN to identify the triangle cells representing buildings, and the edges coinciding with the footprint polygons were designated as walls. Supplementary Fig. 21 provides an illustration of the process for the Warren region to demonstrate this procedure. The simplification of building footprints was necessary for two main reasons: (1) to prevent the generation of very small triangles - this constraint was imposed to maintain an appropriate time step in the finite-volume method implemented in OFM for simulating overland flow; and (2) to reduce the number of cells in the overall mesh representing the watershed, thereby reducing the computational burden of the numerical simulation.

Overall, the TIN resulted in 116,215 mesh nodes and 232,292 triangle cells (Supplementary Fig. 19b). The smallest cell area is 1.3 m² while the average cell size generated for the Warren area is about 47 m². It is worth noting that, even with the this modestly sized TIN, the simulation time for a 24-hour rainfall event requires up to 240 hours of wall-clock time to complete. It should be noted that in our study, technologies to speed up model runtime, such as parallelization or the use of surrogate modeling ⁵⁵, were not employed. However, when such computationally expensive models need to be used in applications such as design optimization and control/operation of stormwater systems, as well as real-time forecasting, such technologies are particularly necessary to provide simulation/forecast results in a timely manner.

All of the land cover is developed area with the impervious surface ranging from 47% to 95%. Especially for the Warren area, the impervious surface is up to 94.48%. The land use and impervious surface information was downloaded from National Land Cover Database 2019 (https://www.mrlc.gov/).

Experimental design

The research comprised of two modeling experiments to address two research questions. First, the study evaluated two scenarios of the spatial distribution of rainfall in causing flooding within the Warren area. For this purpose, STORM2014 precipitation data were configured as a grid with the resolution of 500m×500m using rainfall data obtained from the DET rain gage. This gridded product was used as model input in the first scenario called "HR-Integrated" (the results are presented in Fig. 2d). The drainage system was designed to closely resemble real-world conditions, allowing for water exchange between the inside and outside of the Warren drainage system based on the dynamically changing distribution of hydraulic head over the surface and below-ground in storm sewers. In the second scenario, the gridded rainfall data for the Warren area were set to 0 mm for the duration of the STORM2014 event (i.e., 24-hour). This scenario was named "NR-Integrated" (Fig. 2e).

In the second experiment, we explore the functioning of two stormwater sewer outfalls (Fig. 2b-c) using three different model configurations. Specifically, the first setup represents the most realistic design by allowing backwater to occur (water from the open channel flows back into the sewer system through the outfall), referred to as the "Integrated" outfalls. The second setup assumes the current sewer system is unaffected by water levels at the outfall locations, maximizing drainage capacity by allowing unrestricted discharge from the stormwater system into the open channel without backflow from Bear Creek, termed "Controlled" outfalls. The third setup precludes any water exchange at the outfalls between stormwater system and open channel, with the total outflow from system stored in an underground storage sized to contain all runoff from the Red Run watershed under the STORM2014 event (with a volume of ~24.77 million m³) rather than entering the open channel. We term this case "Water loss" with results shown in Supplementary Fig. 3.

The Manning's roughness coefficient is the most influential parameter for overland and sewer flows ⁵⁶. For surface flow simulated with the OFM model, we assume a spatially uniform value of 0.015, which is in the middle of the interval for concrete surfaces (0.012–0.018) ²⁹. Manning's coefficients for all conduits are set to 0.013 (with concrete as the pipe material) ⁵⁷.

Data mining and Model evaluation

In terms of its suitability to mimic the important details of hydrodynamic processes such as overland flow, backwater, hydraulic jump, as well as the influence of vegetation and buildings on surface flow, the tRIBS-OFM model has been extensively tested and validated in numerous previous studies ^{53,55,58}. To analyze the performance of the tRIBS-OFM model with respect to its capability of depicting the interaction between the stormwater system and surface flow, we conducted a benchmark experiment to evaluate simulated surcharge in manholes, as demonstrated in Supplementary Fig. 22. A detailed description of this case study is provided by the United Kingdom Environment Agency ⁵⁹. This evidence supports that tRIBS-OFM produces reliable results when simulating complex hydraulic dynamics and interactions between the stormwater system and the surface, comparable with that of other models that used the same dataset ⁵⁹. The competent performance by tRIBS-OFM makes it a great choice for studies of urban flooding.

Due to the limitations of flood data availability in the study area, conventional model validation is not feasible. Therefore, an alternative approach was adopted to validate the model results by collecting flood evidence from various internet sources. The manual process of data collection and analysis involved several steps to ensure reliability and accuracy.

- Keywords & Search operators: An ad-hoc combination of keywords was used for searching, including: "2014 flood," "Macomb County," "Oakland County," "Warren MI," "Bear Creek flood," and "Michigan flood disaster 2014". These keywords were entered into the Google search engine. From the obtained search results, images published in reports, newspapers, and blogs were selected and evaluated for inclusion in the study.
- Quality assessment and metadata extraction: In a subsequent filtering step, the obtained images were visually analyzed to determine flooded locations and water levels relative to visible objects such as people, vehicles, or traffic signs. Details about street names or intersections were used to estimate and extract coordinates. The extracted metadata include

- information such as coordinates, flood severity, flooded location (street name), and the website link from which the image was sourced.
 - Uncertainty assessment: Estimating water levels from images involves subjective interpretation and conjectures necessitating an evaluation of relevant confidence intervals. Typically, there are two approaches to estimate this uncertainty: (1) assuming that the uncertainty is proportional to the estimated water depth, or (2) considering that the uncertainty is associated with each reference class ⁶⁰. In this study, we opted for the first approach, assuming that the standard deviation is equal to 20% of the estimated water depth. The final results for the estimation of water levels at six locations are described in Supplementary Table 2.

The flood depth data were subsequently used to validate the model results (Supplementary Fig. 23). One limitation of these flood depth estimations is the lack of certain information regarding the time at which the images were acquired. Therefore, accuracy of such a comparison of the model results is constrained. Consequently, we considered the obtained flood depths as a threshold for "being flooded" and use them to compare with the model results to determine whether the model exceeds this threshold at any simulation time. In essence, the model results confirm that at the locations marked as "flooded", the occurrence of flooding is consistent with the simulation results, with relatively minor discrepancies in flood depths. For example, at location 1, the model yields a maximum flood depth of approximately 0.85 m, while the estimated data range from 0.8 to 1.2 m. Similar results can be observed for other locations.

Fundamentally, an accurate description of what occurs in reality requires significant efforts not only in terms of the model's capabilities but also regarding the accuracy of the data used. This study does not aim to assert that the model used in the study can precisely depict all relevant flood dynamics during the STORM2014 across the entire study area (Red Run watershed and Warren area). Rather, we aim to portray that in conditions of complex permutation of the stormwater infrastructure, terrain, landuse, or building, the sophisticated, state-of-the-science model can provide insights into potential flood phenomena that have not been previously examined.

Data availability

The land use cover was obtained from the National Land Cover Database 2019 (https://www.mrlc.gov). High-resolution elevation data was provided by the USGS, https://apps.nationalmap.gov/downloader/). The building footprint data was obtained from the Southeast Michigan Council of Governments (https://maps.semcog.org/BuildingFootprints). Data on the stormwater system, including manholes, outfalls, and pipes, were collected and compiled in collaboration with the Macomb and Oakland Counties. The rainfall data were the Automated Surface Observing Systems network (https://www.weather.gov/asos/). The simulation dataset (approximately 600 Gigabytes) archived on the Globus Cloud is available upon written request to the authors.

Code availability

- Data processing and analysis were performed using MATLAB 2022b (standard version). The
- 594 source code is publicly accessible via GitHub at
- 595 https://github.com/vinhngoctran/RedRun_processing.

596 Acknowledgements

- V. N. Tran and V. Y. Ivanov acknowledge the support of the U.S. National Science Foundation
- 598 CMMI program award # 2053429 and the Department of Defense, Department of the Navy, the
- 599 Office of Naval Research award # N00014-23-1-2735. Authors acknowledge informative
- discussions with P. Seelbach, B. Kerkez, J. Bednar, G. O'Neil, C. Brown, C. Purdy, A. Asher, M.
- Thomas, and S. Bergt that assisted this study.

Author Contribution Statement

- Authors and Affiliations
- Department of Civil and Environmental Engineering, University of Michigan, Ann Arbor, MI
- 605 48109, USA
- Vinh Ngoc Tran, Valeriy Y. Ivanov, Weichen Huang, and Kevin Murphy
- Ocean and Hydrologic Modeler at National Oceanic and Atmospheric Administration (NOAA)
- National Ocean Service, Office of Coast Survey (NOS/OCS), Silver Spring, MD 20910, USA
- Ocean and Hydrologic Modeler at Earth Resources Technology (ERT), Laurel, MD 20707, USA
- 610 Fariborz Daneshvar
- Macomb County Public Works Commissioner Candice S. Miller, Clinton Township, MI 48036,
- 612 USA
- 613 Jeff H. Bednar
- Department of Civil and Environmental Engineering, University of Wisconsin-Madison, Madison,
- 615 WI 53706, USA
- 616 G. Aaron Alexander and Daniel B. Wright
- School of Civil and Environmental Engineering, University of Ulsan, Ulsan 44600, South Korea
- 618 Jongho Kim

619 Contributions

- V.N.T and V.Y.I designed the study. V.N.T, W.H, K.M, and F.D collected the data. V.N.T
- 621 conducted the experiments. V.N.T and V.Y.I analyzed the data and wrote and revised the
- 622 manuscript with inputs from all co-authors. All authors contributed to the interpretation of results,
- writing and revision of the paper.

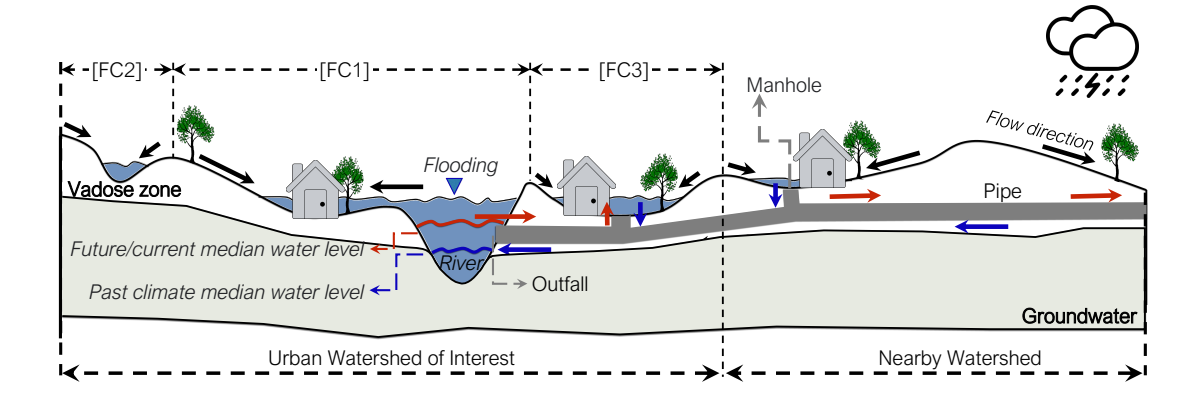
624 Corresponding author

625 Correspondence to Valeriy Y. Ivanov.

Competing Interests Statement

The authors declare no competing interests.

Figure captions



629

630

631

632

633

634

635

636

637

638

639

640

641

642

643

644

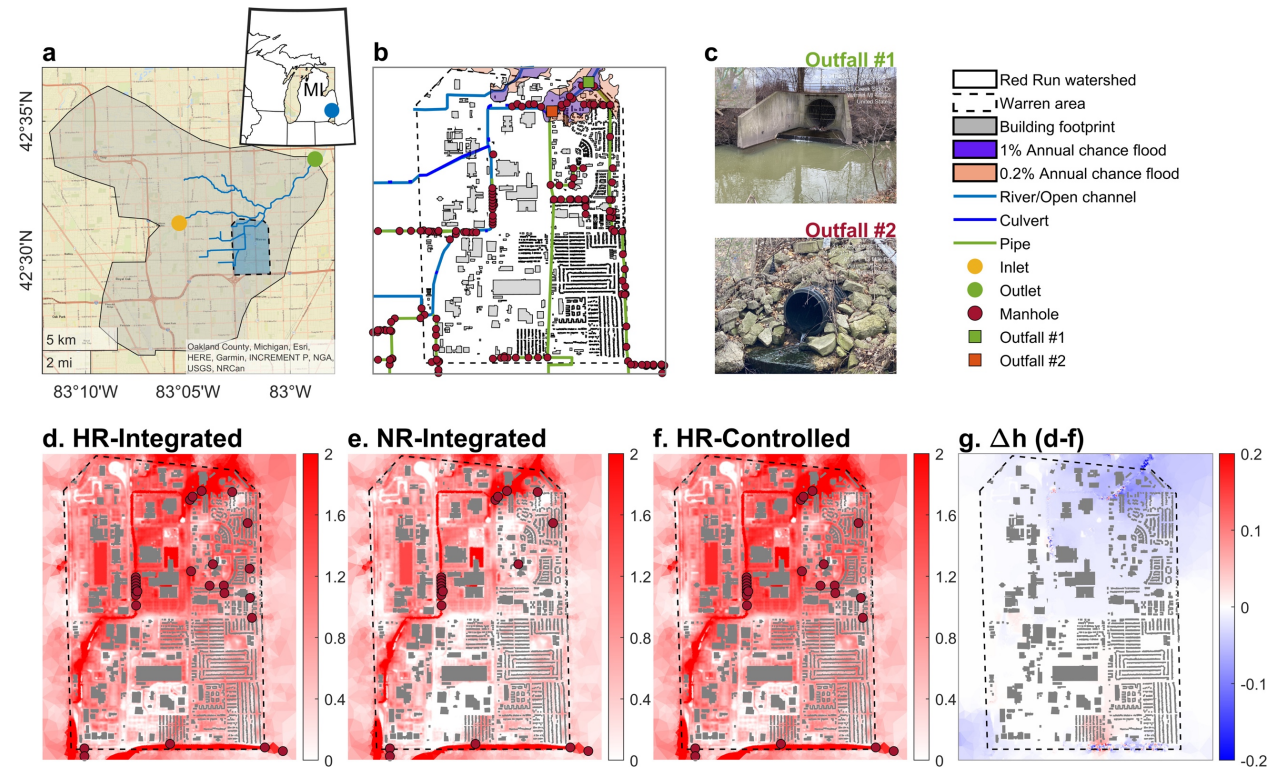
645

646

647

626

Figure 1. Illustration of key urban flooding concepts (FCs). A cross-section of an urban watershed depicts residential areas (buildings), green spaces (trees), an open channel (rive crosssection), and an underground stormwater system (manholes, pipes, and outfalls). Outfall discharging into the river connects the urban stormwater network with a larger drainage system. The arrows indicate potential flow directions of water. Black arrows indicate surface flow directions, blue arrows show flows from the ground surface into the sewer system and out the outfall locations (e.g., open channels), while red arrows depict backwater occurrences when open channel flows reverse into the drainage system through outfalls, potentially causing surcharging at manholes. The blue curved line represents normal water level (historical conditions), while the red curve represents the current or future river water level due to the influence of climate change and urbanization. FC1 represents flooding due to high water levels in the river, causing overflow and inundation of the surrounding floodplain (river-induced, or "fluvial" flooding). FC2 represents flooding caused by intense rainfall and insufficient natural or engineered drainage capacity of the area (rainfall-induced or "pluvial" flooding). FC3 represents flooding caused by the hydraulic connection of stormwater infrastructure with stream channels and other drainage basins. FC3 flooding can be caused by water accumulation due to either fluvial or pluvial flooding or backup flow from the river through drainage pipes, leading to surcharge at the manholes (infrastructure-induced flooding).



650

651

652

653

654

655

656

657

658

659

660

661

662

663

664

665

666

667

668

Figure 2. Flood maps of Warren, Michigan for STORM2014 (August 11, 2014) event. The Warren area specified with the dashed line in (b) is situated in the Red Run watershed (a) in southeastern Michigan. The orange and green dots in (a) indicate the inlet and outlet locations of the watershed, with the inlet being the discharge point of the George W. Kuhn Retention Treatment Basin. Subplot (b) illustrates the Warren area, including buildings (grey polygons), open channels (e.g., Bear Creek), culverts (dark blue lines), underground pipes (green lines), manholes (brown dots), and two outfalls (green and red squares). The outfalls are shown in photographs in (c). The blue and orange areas in (b) represent the regions at risk of flooding with a 1% and 0.2% annual chance flood, respectively, provided by FEMA. Subplot (d) displays the simulation results for the maximum inundation depth of the flood event using STORM2014, where the land cover conditions and culvert systems closely reproduce actual drainage conditions, allowing for both drainage and backwater phenomena at the outfalls (referred to as the "integrated" outfall condition). The rainfall is uniformly distributed across the entire Red Run watershed in this scenario (referred to as homogeneous rain or HR). Subplot (e) illustrates the maximum inundation depth results for a simulation configuration that mimics that of (d), but with rain occurring only *outside* of the Warren area (referred to as no-rain or NR). Subplot (f) shows the maximum inundation depth results using HR, but assuming that all water collected by storm sewers discharges into the open channel, i.e., backwater effect in drainage pipes is not enabled (referred to as the HR "controlled" outfall). Subplot (g) presents the difference of flood depths in (d) and (f). The locations of surcharging manholes in (d)-(f) are shown with brown dots. The values presented in (d)-(g) are expressed in meters.

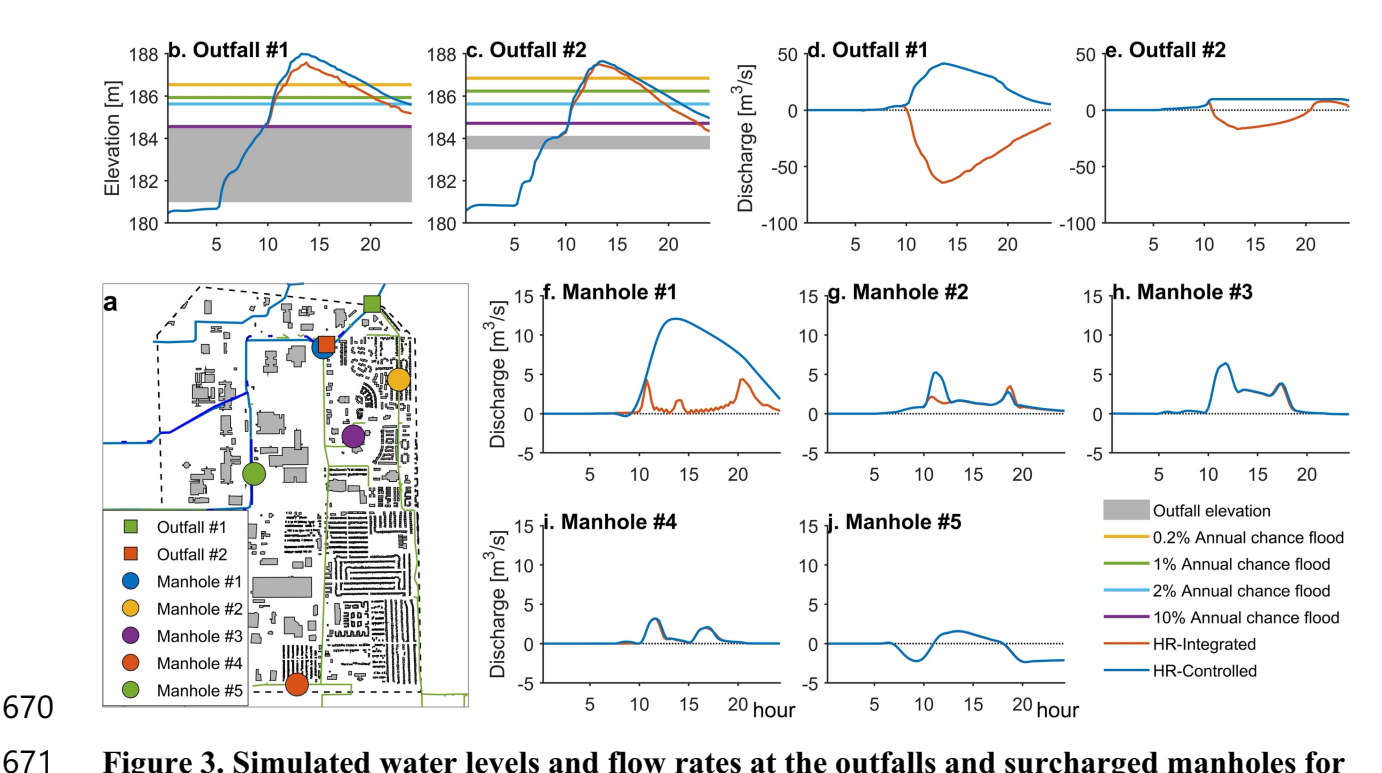


Figure 3. Simulated water levels and flow rates at the outfalls and surcharged manholes for STORM2014. Map (a) depicts the locations of outfalls and select manholes with results shown in subplots (b-j). Subplots (b) and (c) display the simulated water surface elevations at two outfall locations (see the legend). The grey region represents invert (pipe bottom-to-top) elevation range of the outfalls. The colored lines represent the floodwater levels at probabilities ranging from 10% to 0.2% annual chance flood as provided by FEMA. Subplots (d) and (e) illustrate the outflow (positive values) or inflow (negative values) rates at the outfalls for the HR-Integrated and HR-Controlled scenarios. Subplots (f) to (j) present the overflow (positive) and drainage (negative) rates for five manholes indicated by circles in (a).

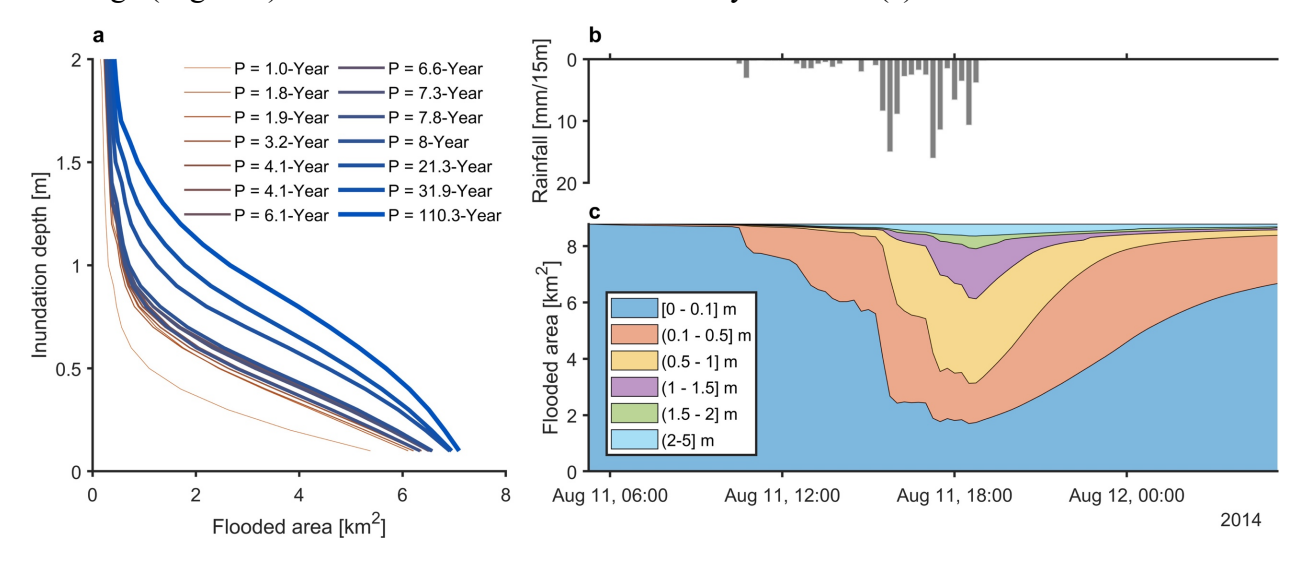


Figure 4. A relationship between flood inundation and flooded area. Subplot (a) shows a relationship between the flooded Warren area and the maximum flood level calculated for the 14

- largest rainfall events for the Warren area between 2009 and 2021 (see Supplementary Fig. 4).
- The legend indicates the rainfall frequency (return period P) for each event, which is calculated
- based on the maximum rainfall within 3 hours and uses the intensity-duration-frequency (IDF)
- 686 curve provided by NOAA. Subplots (b) and (c) respectively illustrate the rainfall time series and
- the flooded area for six flood levels during the STORM2014 event (the return period is 110.3
- 688 years).

References

- Donat, M. G., Lowry, A. L., Alexander, L. V., O'Gorman, P. A. & Maher, N. More extreme precipitation in the world's dry and wet regions. *Nature Climate Change* **6**, 508-513, doi:10.1038/nclimate2941 (2016).
- Prein, A. F. *et al.* The future intensification of hourly precipitation extremes. *Nature Climate Change* **7**, 48-52, doi:10.1038/nclimate3168 (2016).
- 695 3 Scott, D. T., Gomez-Velez, J. D., Jones, C. N. & Harvey, J. W. Floodplain inundation 696 spectrum across the United States. *Nat Commun* **10**, 5194, doi:10.1038/s41467-019-697 13184-4 (2019).
- 4 Paprotny, D., Sebastian, A., Morales-Napoles, O. & Jonkman, S. N. Trends in flood
 losses in Europe over the past 150 years. *Nat Commun* 9, 1985, doi:10.1038/s41467-018-04253-1 (2018).
- 701 5 UNDRR. UNDRR Annual report 2021. (United Nations Office for Disaster Risk
 702 Reduction, 2021).
- 703 6 NWS. NWS Preliminary US Flood Fatality Statistics. (2023).
- 704 7 NOAA. Storm Events Database. (2023).
- NCEI. US Billion-Dollar Weather and Climate Disasters. *NOAA National Centers for Environmental Information*, doi:https://www.doi.org/10.25921/stkw-7w73 (2023).
- 707 9 Hirabayashi, Y. *et al.* Global flood risk under climate change. *Nature climate change* **3**, 816-821 (2013).
- 709 10 Rentschler, J. *et al.* Global evidence of rapid urban growth in flood zones since 1985. 710 *Nature* **622**, 87-92, doi:10.1038/s41586-023-06468-9 (2023).
- 711 Revi, A. et al. Chapter 8. Urban Areas. Climate Change 2014: Impacts, Adaptation, and 712 Vulnerability. Part A: Global and Sectoral Aspects. Contribution of Working Group II to 713 the Fifth Assessment Report of the Intergovernmental Panel on Climate Change, 535-612 714 (2014).
- Nowak, D. J. & Walton, J. T. Projected urban growth (2000–2050) and its estimated impact on the US forest resource. *Journal of Forestry* **103**, 383-389 (2005).
- 717 13 Andreadis, K. M. *et al.* Urbanizing the floodplain: global changes of imperviousness in flood-prone areas. *Environmental Research Letters* **17**, 104024, doi:10.1088/1748-719 9326/ac9197 (2022).
- Golden, H. & Hoghooghi, N. Green infrastructure and its catchment-scale effects: an emerging science. *WIREs Water* 1, e1254, doi:https://doi.org/10.1002/wat2.1254 (2018).
- Radhakrishnan, M., Pathirana, A., Ashley, R. M., Gersonius, B. & Zevenbergen, C. Flexible adaptation planning for water sensitive cities. *Cities* **78**, 87-95 (2018).
- Wong, T. H. & Brown, R. R. The water sensitive city: principles for practice. *Water science and technology* **60**, 673-682 (2009).

- 726 17 EPA. EPA Science Matters Newsletter: From Gray to Green Helping Communities
 727 Adopt Green Infrastructure. (2023).
- Alves, A., Vojinovic, Z., Kapelan, Z., Sanchez, A. & Gersonius, B. Exploring trade-offs among the multiple benefits of green-blue-grey infrastructure for urban flood mitigation.

 Science of The Total Environment 703, 134980,
 doi:https://doi.org/10.1016/j.scitotenv.2019.134980 (2020).
- Wilbanks, T. et al. in And Vulnerabilities: Technical Report for the US Department of Energy in Support of the National Climate Assessment (Springer, 2013).
- Collentine, D. & Futter, M. N. Realising the potential of natural water retention measures in catchment flood management: trade-offs and matching interests. *Journal of Flood Risk Management* **11**, 76-84, doi:https://doi.org/10.1111/jfr3.12269 (2018).
- FAR EFAB Report: Evaluating Stormwater Infrastructure Funding and Financing. (2023).
- Qiao, X.-J., Kristoffersson, A. & Randrup, T. B. Challenges to implementing urban
 sustainable stormwater management from a governance perspective: A literature review.
 Journal of Cleaner Production 196, 943-952,
 doi:https://doi.org/10.1016/j.jclepro.2018.06.049 (2018).
- Rosenzweig, B. R. *et al.* Pluvial flood risk and opportunities for resilience. *WIREs Water* 5, e1302, doi:https://doi.org/10.1002/wat2.1302 (2018).
- ten Veldhuis, J. A. E. How the choice of flood damage metrics influences urban flood risk assessment. *Journal of Flood Risk Management* 4, 281-287,
 doi:https://doi.org/10.1111/j.1753-318X.2011.01112.x (2011).
- Packhaus, A., Dam, T. & Jensen, M. B. Stormwater management challenges as revealed through a design experiment with professional landscape architects. *Urban Water Journal* 9, 29-43 (2012).
- Wright, D. B., Bosma, C. D. & Lopez-Cantu, T. U.S. Hydrologic Design Standards
 Insufficient Due to Large Increases in Frequency of Rainfall Extremes. *Geophysical Research Letters* 46, 8144-8153, doi:https://doi.org/10.1029/2019GL083235 (2019).
- 754 27 Mays, L. W. Stormwater collection systems design handbook. (McGraw-Hill Education, 2001).
- ASCE. Standard guidelines for the design of urban stormwater systems. (2006).
- 757 29 Arcement, G. J. & Schneider, V. R. Guide for selecting Manning's roughness coefficients for natural channels and flood plains. (1989).
- 759 30 CIRIA, D. The SUDS manual. CIRIA, London (2007).
- Department, D. S. *Stormwater Drainage Manual: Planning, Design and Management.*(Government of the Hong Kong Special Administrative Region Hong Kong, 2018).
- 762 32 Argue, J. *et al.* Water sensitive urban design: basic procedures for 'source control' of stormwater. *Urban water resource centre, University of South Australia, Adelaide* (2004).
- Bradford, A. & Gharabaghi, B. Evolution of Ontario's Stormwater Management Planning
 and Design Guidance. *Water Quality Research Journal* 39, 343-355,
 doi:10.2166/wqrj.2004.047 (2004).
- 768 34 Wing, O. E. J. *et al.* Inequitable patterns of US flood risk in the Anthropocene. *Nature Climate Change* **12**, 156-162, doi:10.1038/s41558-021-01265-6 (2022).
- 770 35 National Academies of Sciences, E. & Medicine. *Framing the challenge of urban flooding in the United States.* (National Academies Press, 2019).

- 772 36 Rosenzweig, B. R. *et al.* The Value of Urban Flood Modeling. *Earth's Future* **9**, doi:10.1029/2020ef001739 (2021).
- 774 37 Guo, K., Guan, M. & Yu, D. Urban surface water flood modelling a comprehensive review of current models and future challenges. *Hydrol. Earth Syst. Sci.*, doi:https://doi.org/10.5194/hess-25-2843-2021 (2021).
- Forero-Ortiz, E., Martínez-Gomariz, E. & Cañas Porcuna, M. A review of flood impact assessment approaches for underground infrastructures in urban areas: a focus on transport systems. *Hydrological Sciences Journal* **65**, 1943-1955, doi:10.1080/02626667.2020.1784424 (2020).
- 781 39 Carmichael, C., Danks, C. & Vatovec, C. Assigning blame: How local narratives shape
 782 community responses to extreme flooding events in Detroit, Michigan and Waterbury,
 783 Vermont. *Environmental Communication* 14, 300-315 (2020).
- 784 40 Shepardson, D. White House approves Michigan disaster declaration. *Detroit News Washington Bureau* (2014).
- 786 41 FEMA. National Flood Hazard Layer. (2023).
- Yazdanfar, Z. & Sharma, A. Urban drainage system planning and design challenges
 with climate change and urbanization: a review. *Water Science and Technology* 72, 165-179, doi:10.2166/wst.2015.207 (2015).
- 790 43 Chen, S. S. *et al.* Designing sustainable drainage systems in subtropical cities: Challenges and opportunities. *Journal of Cleaner Production* **280**, 124418, doi:https://doi.org/10.1016/j.jclepro.2020.124418 (2021).
- Yazdanfar, Z. & Sharma, A. Urban drainage system planning and design—challenges with climate change and urbanization: a review. *Water Science and Technology* **72**, 165-179 (2015).
- Schmitt, T. G. & Scheid, C. Evaluation and communication of pluvial flood risks in urban areas. *WIREs Water* 7, e1401, doi:https://doi.org/10.1002/wat2.1401 (2020).
- Prosdocimi, I., Kjeldsen, T. R. & Miller, J. D. Detection and attribution of urbanization effect on flood extremes using nonstationary flood-frequency models. *Water Resources Research* **51**, 4244-4262, doi:https://doi.org/10.1002/2015WR017065 (2015).
- 803 48 Council, N. R. *Mapping the zone: Improving flood map accuracy*. (National Academies Press, 2009).
- Kousky, C. Financing flood losses: A discussion of the national flood insurance program. *Risk Management and Insurance Review* **21**, 11-32 (2018).
- Pralle, S. Drawing lines: FEMA and the politics of mapping flood zones. *Climatic Change* **152**, 227-237 (2019).
- Ivanov, V. Y., Vivoni, E. R., Bras, R. L. & Entekhabi, D. Catchment hydrologic response with a fully distributed triangulated irregular network model. *Water Resources Research* **40**, doi:10.1029/2004wr003218 (2004).
- Ivanov, V. Y., Vivoni, E. R., Bras, R. L. & Entekhabi, D. Preserving high-resolution surface and rainfall data in operational-scale basin hydrology: a fully-distributed
- physically-based approach. *Journal of Hydrology* **298**, 80-111,
- 815 doi:https://doi.org/10.1016/j.jhydrol.2004.03.041 (2004).

- Kim, J., Warnock, A., Ivanov, V. Y. & Katopodes, N. D. Coupled modeling of hydrologic and hydrodynamic processes including overland and channel flow. *Advances in Water Resources* **37**, 104-126, doi:10.1016/j.advwatres.2011.11.009 (2012).
- Rossman, L. A. *Storm water management model user's manual, version 5.0.* (National Risk Management Research Laboratory, Office of Research and ..., 2010).
- Ivanov, V. Y. *et al.* Breaking Down the Computational Barriers to Real-Time Urban
 Flood Forecasting. *Geophysical Research Letters*, doi:10.1029/2021gl093585 (2021).
- Ozdemir, H., Sampson, C. C., de Almeida, G. A. M. & Bates, P. D. Evaluating scale and roughness effects in urban flood modelling using terrestrial LIDAR data. *Hydrol. Earth Syst. Sci.* 17, 4015-4030, doi:10.5194/hess-17-4015-2013 (2013).
- 826 57 Chow, V. Open channel hydraulics. MCGraw Hiu (1959).

- Kim, J., Ivanov, V. Y. & Katopodes, N. D. Hydraulic resistance to overland flow on surfaces with partially submerged vegetation. *Water Resources Research* **48**, doi:10.1029/2012wr012047 (2012).
- Néelz, S. & Pender, G. Benchmarking the latest generation of 2D hydraulic modelling packages. *Environment Agency: Bristol, UK* (2013).
- Songchon, C., Wright, G. & Beevers, L. The use of crowdsourced social media data to improve flood forecasting. *Journal of Hydrology* **622**, 129703, doi:https://doi.org/10.1016/j.jhydrol.2023.129703 (2023).